**Electronic supplementary information (ESI) for the manuscript:**

# Highly active Au–Pd nanoparticles supported on three-dimensional graphene–carbon nanotube hybrid for selective oxidation of methanol to methyl formate

Ruiyi Wang,[ab] Zhiwei Wu,[a] Guofu Wang,[a] Zhangfeng Qin,[*a] Chengmeng Chen,[c] Mei Dong,[a] Huaqing Zhu,[a] Weibin Fan[a] and Jianguo Wang[*a]

[a] *State Key Laboratory of Coal Conversion, Institute of Coal Chemistry, Chinese Academy of Sciences, P.O. Box 165, Taiyuan, Shanxi 030001, PR China. E-mail: qzhf@sxicc.ac.cn (Z. Qin); iccjgw@sxicc.ac.cn (J. Wang)*

[b] *University of Chinese Academy of Sciences, Beijing 100049, PR China*

[c] *Key Laboratory of Carbon Materials, Institute of Coal Chemistry, Chinese Academy of Sciences, P.O. Box 165, Taiyuan, Shanxi 030001, PR China*

## 1. More Experimental Details:

*1.1. Catalyst Preparation*

**Preparation of graphene oxide (GO).** GO was synthesized by a modified Hummers'

[*] Corresponding authors. Tel.: +86-351-4046092; Fax: +86-351-4041153.
*E-mail address:* qzhf@sxicc.ac.cn (Z. Qin); iccjgw@sxicc.ac.cn (J. Wang)

*Postal Address:* Prof. Jianguo WANG
State Key Laboratory of Coal Conversion
Institute of Coal Chemistry, Chinese Academy of Sciences
P. O. Box 165
Taiyuan, Shanxi 030001
PR China

method.[1] Briefly, graphite powder (10 g) and sodium nitrate (5 g) were mixed with sulfuric acid (98 wt.%, 230 mL) in a beaker immersed in an ice-water bath with agitation. Potassium permanganate (30 g) was then added slowly to the mixture and the resultant mixture was kept at 35±2 °C for 30 min. After that, deionized water (460 mL) was added gradually; the temperature of the water bath was then increased to 98 °C and maintained at this temperature for 40 min. The resultant bright-yellow suspension was then diluted and further treated with $H_2O_2$ solution (30%, 30 mL). Finally, the suspension was centrifuged and washed carefully to remove the residual salt, and then dewatered at 50 °C under vacuum to obtain the graphite oxide powder. Graphene oxide was then obtained by exfoliating the graphite oxide in aqueous solution under sonication for 2 h, and followed by a vacuum drying process.

**Preparation of graphene (Gr).** Graphene used here was obtained by rapid heating-up of the above-obtained graphene oxide under high vacuum.[2] The as-prepared GO was grounded into fine powder (300 mesh) and loaded into a quartz tube. It was then evacuated to a pressure lower than 2.0 Pa and heated quickly to 200 °C at a rate of 30 °C $min^{-1}$; the graphene sample of fluffy black powder was then generated through the abrupt expansion of GO at about 200 °C.

**Preparation of graphene–carbon nanotubes (Gr–CNT) hybrid.** The Gr–CNT hybrids were obtained by the solution self-assemble method, i.e. by sonicating the aqueous colloidal suspensions of graphene oxide and acid-functionalized CNT (Fig. S1). Briefly, CNT (purchased from Chengdu Organic Chemicals Co. Ltd., Chinese Academy of Sciences) were first functionalized by refluxing in $H_2SO_4$ and $HNO_3$ for 4 h, filtered and washed with deionized water, and then dried in vacuum. Meanwhile, the graphene oxide prepared in advance was dispersed in deionized water. The functionalized CNT were then poured into the aqueous colloidal suspensions of graphene oxide and the mixture was sonicated for 2 h to

finish the self-assembling. After that, fresh $NaBH_4$ aqueous solution was added into the mixture and the mixture was stirred at 70 °C for 1 h. Finally, the Gr–CNT hybrids were collected by centrifuging for 10 min at 6000 rpm. The resultant Gr–CNT hybrids are denoted as Gr–CNT($w$), where $w$ is the mass ratio of graphene to carbon nanotubes ($w$ = 1–5 in this work).

{Fig. S1}

**Preparation of Gr–CNT hybrid supported gold-palladium (Au–Pd/Gr–CNT) catalysts.** With Gr–CNT as the support, Au–Pd/Gr–CNT catalysts were prepared through the deposition–precipitation method with $HAuCl_4 \cdot 3H_2O$ and $PdCl_2$ as precursors; the loadings of Au and Pd for all supported Au–Pd catalysts were designed to be 2 and 1 wt.%, respectively. Typically, Gr–CNT support (200 mg) was dispersed in an aqueous solution of sodium carbonate (80 mL) situated in a water bath of 60 °C; after stirring for 20 min, a mixed aqueous solution of $HAuCl_4 \cdot 3H_2O$ and $PdCl_2$ was added dropwisely. The mixture was then stirred rigorously for 2.5 h; the Au–Pd/Gr–CNT catalysts were filtered and washed with deionized water until no $Cl^-$ was detected by $AgNO_3$ solution. After that, the Au–Pd/Gr–CNT catalysts were dried at 120 °C in vacuum for 3 h and then calcined at 200 °C in air for another 3 h.

**Preparation of gold-palladium catalysts supported on Graphene and CNT.** For comparison, other Au–Pd catalysts supported on graphene (Au–Pd/Graphene), carbon nanotubes (Au–Pd/CNT), etc., were also prepared in a similar way.[3] In this work, the loadings of Au and Pd for all supported Au–Pd catalysts were controlled as 2 and 1 wt.%, respectively. The actual loadings of Au and Pd for the supported Au–Pd catalysts were also determined by inductively coupled plasma atomic emission spectroscopy (ICP-AES) on a Thermo iCAP 6300 ICP-OES with a CID detector.

*1.2. Catalyst Characterization*

The transmission electron microscopy (TEM) and high-resolution transmission electron microscopy (HRTEM) images of the catalysts were obtained on a JEM 2010 microscope operated at 200 kV. The mean particle size is estimated from a statistic result of 100 particles randomly selected in the image.

The scanning electron microscopy (SEM) images to characterize the surface morphologies of the as-prepared samples were acquired on a field emission scanning electron microscope (FESEM, JSM 7001-F, JEOL, Japan), with energy dispersive X-ray spectroscopy (EDX) (QX200).

The powder X-ray diffraction (XRD) patterns of the catalysts were collected on a Rigaku MiniFlex II desktop X-ray diffractometer with Cu Kα radiation source. The measurements were made in the $2\theta$ range from 5° to 80° with a scanning rate of 4 min$^{-1}$.

The X-ray photoelectron spectroscopy (XPS) spectra were taken on a Thermo ESCALAB 250 instrument, with an Al Kα monochromator X-rays source ($h\gamma$ = 1486.6 eV); approximate 150 mg of the powder sample was compressed into a wafer for the measurements. The detailed spectra in the Au 4f and Pd 3d regions were measured in the ranges of 80–93 and 330–350 eV, respectively.

The nitrogen sorption isotherms were measured at −195.7 °C on a physisorption analyzer (ASAP 2000, Micromeritics Instrument Co., USA). The catalyst samples were degassed under high vacuum at 300 °C for 8 h prior to the measurement. The surface area was calculated from the adsorption branch in the range of relative pressure from 0.05 to 0.25 by Brunauer–Emmett–Teller (BET) method and the pore size distribution was derived from the adsorption branch by Barrett-Joyner-Halenda (BJH) method; the pore volume was estimated

at a relative pressure of 0.99.[4]

X-ray absorption near-edge spectroscopy (XANES) measurements were performed at the beam line BL14W1 of Shanghai Synchrotron Radiation Facility, China. Pd K-edge X-ray absorption spectra were collected at room temperature in the fluorescence mode using a solid state detector and the XANES data were processed and fitted by using the IFEFFIT package.

*1.2. Catalytic Test and Analytical Procedures*

The catalytic performance of various catalysts in methanol (MeOH) oxidation was tested in a quartz fixed-bed microreactor with an inner diameter of 6 mm, as illustrated in Fig. S2. Methanol was introduced into the reactor by bubbling argon via a glass saturator filled with methanol kept at 30 °C. Oxygen was then mixed with the argon stream carrying methanol vapor outflow of the saturator. In each test, 0.06 g catalyst mixed with 1 mL quartz sand was loaded. The feed stream consisted of 6.4 vol.% $CH_3OH$, 70.2 vol.% $O_2$, and balanced argon, with a flow rate of 42.8 mL $min^{-1}$, equivalent to a gas hourly space velocity (GHSV) of 42,800 mL $g^{-1}$ $h^{-1}$.

The products were analyzed on-line by a gas chromatography (GC) equipped with a Porapak-T column and a thermal conductivity detector (TCD). The gas lines were kept at 110 °C to prevent any reactants and products from condensation (Fig. S2)

**{Fig. S2}**

The products consist of $CH_3OH$, MF and $CO_2$. The conversion of methanol $x_{MeOH}$ is determined by

$$x_{MeOH} = (n_{MeOH,feed} - n_{MeOH,outlet})/n_{MeOH,feed} \times 100\% \tag{1}$$

and the selectivity to each product ($s_i$) is determined by

$$s_i = (n_{i,\text{outlet}} \times k_i)/(n_{\text{MeOH,feed}} - n_{\text{MeOH,outlet}}) \times 100\% \qquad (2)$$

where $k_i$ is the carbon number in one molecule of product $i$.

Turnover frequency (TOF, h$^{-1}$), the number of MF molecules formed per active site and hour, is estimated on the basis of total Au and Pd atoms, which is calculated from the loadings of Au plus Pd, i.e.,

$$\text{TOF} = \frac{[\text{Product molecules}]}{[\text{Number of active sites}] \times [\text{Time}]} = \frac{0.5 \times F_{\text{MeOH}} \times x_{\text{MeOH}} \times s_{\text{MF}}}{60 \times 22400 \times w_{\text{cat}} \times N_{\text{Au\&Pd}}} \qquad (3)$$

where $F_{\text{MeOH}}$ is the volume flow rate of methanol (in unit of mL min$^{-1}$) and $w_{\text{cat}}$ means the mass of the catalyst loaded in the reactor (in the unit of g) and $N_{\text{Au\&Pd}}$ (g$^{-1}$) means the number of Au and Pd atoms in per gram catalyst.

Thus, the TOF value can be estimated by

$$\text{TOF} = \frac{0.5 \times F_{\text{MeOH}} \times x_{\text{MeOH}} \times s_{\text{MF}}}{60 \times 22400 \times w_{\text{cat}} \times \left( L_{\text{Au}}/M_{\text{Au}} + L_{\text{Pd}}/M_{\text{Pd}} \right)} \qquad (4)$$

where $L_{\text{Au}}$ and $L_{\text{Pd}}$ are the loadings of Au and Pd in wt.%, respectively, while $M_{\text{Au}}$ and $M_{\text{Pd}}$ are the molar masses of Au and Pd, respectively.

## 2. More Results of Catalyst Characterization and Reaction Tests:

### 2.1. More Catalyst Characterization Results

**Actual loadings of Au and Pd.** The actual loadings of Au and Pd on the Au–Pd/CNT, Au–Pd/Graphene and Au–Pd/Gr–CNT($w$) catalysts were also determined by inductively

coupled plasma atomic emission spectroscopy (ICP-AES), as given in Table S1, which proves that the actual loadings of Au and Pd are very close to the designed values and the loss of Au and Pd is negligible upon the aqueous rinsing during the catalyst preparation.

**{Table S1}**

**Textural properties.** The textural properties of carbon nanotubes (CNT), graphene (Gr), Gr–CNT hybrids, and corresponding Au–Pd supported catalysts were measured by nitrogen physisorption, as shown in Fig. S3. Although graphene sheets may have a theoretical surface area of 2600 $m^2$ $g^{-1}$, the surface area of graphene used in this work is only about 218.8 $m^2$ $g^{-1}$, due to the face to face aggregation of graphene sheets. After doping graphene with CNT (186.4 $m^2$ $g^{-1}$), the resultant Gr–CNT(5) hybrid displays a surface area of 311.6 $m^2$ $g^{-1}$, which is much higher than that of either graphene or carbon nanotubes, suggesting that the aggregation of graphene sheets is effectively inhibited by the incorporation of CNT as a spacing inserter. A series of Gr–CNT(*w*) hybrids with different Gr/CNT mass ratios all display a sorption isotherm of type IV with a hysteresis loop according to the IUPAC classification, meaning that they have a mesoporous structure; moreover, a Gr/CNT mass ratio of 5 gives the best doping effect, viz., the highest surface area and mesopore volume. Table 1 in the main manuscript also illustrates that after the loading of Au–Pd nanoparticles, the surface areas of Au–Pd catalysts are only slightly decreased, compared with the corresponding supports, suggesting that the deposition-precipitation process has little effect on the carbonaceous supports.

**{Fig. S3}**

**HRTEM result of Au–Pd/Gr–CNT(5).** The graphene and Gr–CNT hybrid supports used here were provided with a high density of oxygen-containing functionalities (e.g.

hydroxyl, epoxy, carboxyl and carbonyl groups) on the surface;[5] the functionalized groups can enhance the hydrophilicity of graphene, which is of benefit to get a uniform dispersion of metal nanoparticles on the surface of the graphene support.[6]

For Au–Pd/Gr–CNT(5), the SEM results in the main manuscript show that carbon nanotubes are uniformly inserted into the two layers of graphene nanosheets, suggesting that the three dimension Gr–CNT hybrids are formed by the solution self-assemble method. The TEM result indicates that spherical Au–Pd nanoparticles are uniformly dispersed on the surface of Gr–CNT hybrids. The HRTEM image of the Au–Pd/Gr–CNT(5) catalyst shown in Fig. S3 clearly illustrates that gold-palladium nanoparticles with a size of 3–5 nm are mainly anchored on the interfaces of carbon nanotubes and graphene nanosheets; a d-spacing of 0.230 nm are further identified, suggesting the formation of AuPd alloy (d-spacing of 0.235 nm for Au(111) and 0.221 nm for Pd(111)). The doping of graphene with CNT is propitious to reduce the size of metal particles dispersed on the hybrid support, owing to the high surface area and confined space of Gr–CNT hybrids. Moreover, as the Au–Pd particle size in Au–Pd/Gr–CNT(5) is greatly reduced, the Au–Pd alloying degree in Au–Pd/Gr–CNT(5) is also enhanced markedly, in comparison with the partial alloying of twined Au–Pd structure in Au–Pd/Graphene.[3]

**{Fig. S4 & Fig. S5}**

**SEM results of Au–Pd/Gr–CNT(*w*).** The SEM images of the Au–Pd/Gr–CNT(*w*) catalysts with different mass ratios of graphene to carbon nanotube are shown in Fig. S4. All catalysts here show that carbon nanotubes are uniformly inserted into the two layers of graphene nanosheets, forming a well-integrated three-dimensional architecture, which can effectively prevent the face to face aggregation of graphene sheets. The corresponding EDX spectrum of Au–Pd/Gr–CNT(5) with Au and Pd signals confirms the presence of Au and Pd

in the catalyst.

**XPS results of Au–Pd/Gr–CNT(5).** The XPS spectra of Au–Pd supported on CNT, graphene and Gr–CNT(5) are shown in Fig. 3 in the main manuscript. Au 4$f$ spectra can be fitted into four peaks: two peaks for Au$^0$ centered at binding energies of 84.0 and 87.6 eV and other two for cationic gold species Au$^{\delta+}$ centered at 85.3 and 89.2 eV.[7] For Pd 3$d$ XPS spectra, the peaks at 335.6 and 340.8 eV are attributed to Pd$^0$ species and the peaks around 338.1 and 343.9 eV are related to Pd$^{2+}$ species. Compared with those of Au–Pd/CNT and Au–Pd/Graphene, the peaks for both Au$^0$ and Pd$^0$ in the XPS spectra of Au–Pd/Gr–CNT(5) are shifted distinctly towards lower binding energies, suggesting that the synergism of Au–Pd bimetallic nanoparticles is enhanced in Au–Pd/Gr–CNT(5). Venezia and coworkers also observed evident shifts of both Au 4$f_{7/2}$ and Pd 3$d$ spectra towards lower binding energies for bimetallic gold-palladium catalysts, compared with monometallic gold and palladium catalysts, indicating an electronic interaction between gold and palladium.[8]

It was considered that CNT inserted between graphene nanosheets may act as a bridge connecting the defects for electron transfer and then improve their conductivity and catalytic activity.[9,10] Moreover, the graphene support is rich in $\pi$ electrons, which can promote the reduction of Pd$^{2+}$ to Pd$^0$ with the help of Au atoms in AuPd alloy.[3] In this work, the XPS results further illustrate that the electron exchange between gold and palladium is greatly enhanced in Au–Pd/Gr–CNT(5) by doping graphene with CNT; the fraction of Pd$^0$ in Au–Pd/Gr–CNT(5) is about 67.3%, much higher than the value of 56.7% in Au–Pd/Graphene (Table S2).

**{Table S2}**

As shown by the Pd K-edge XANES spectra (Fig. 4 in the main manuscript),

Pd/Graphene is similar to PdO reference in the edge, suggesting that $Pd^{2+}$ is the major Pd species in Pd/Graphene. For Au–Pd/Graphene, however, a fraction of $Pd^{2+}$ is reduced to $Pd^0$; after the doping of CNT into graphene, the fraction of $Pd^{2+}$ reduced to $Pd^0$ in Au–Pd/Gr–CNT(5) is even higher. A quantitative analysis with PdO and Pd foil as references (Table S2) illustrates that the fractions of $Pd^0$ in Au–Pd/Gr–CNT(5) and Au–Pd/Graphene are about 75.0% and 61.3%, respectively.

It was considered that both $Pd^0$ and $Pd^{2+}$ may be involved in the catalytic reaction cycles for methanol oxidation; however, CNT inserted in graphene sheets may greatly improve the redox properties of the resultant Au–Pd/Gr–CNT(5) catalyst and then enhance its catalytic activity in methanol oxidation at low temperature. The binding energy shift and the fraction of $Pd^0$ determined by XPS and XAFS is then a reflection of the extent for the synergy between Au and Pd and the redox ability of these supported Au–Pd catalysts, which is related to their catalytic performance. Thus both the XPS and XANES results support that the addition of CNT can improve the conductivity of graphene support, promote the reduction of PdO and formation of AuPd alloy, and eventually enhance the catalytic activity of Au–Pd supported on the Gr–CNT hybrids.

## 2.2. More Catalytic Test Results

The conversion of methanol and selectivity to MF along with the reaction temperature for methanol oxidation over the Au–Pd/Gr–CNT catalysts with different Gr/CNT mass ratios are displayed in Fig. S6. In general, the conversion of methanol increases with an increase of temperature and reaches 100% at 85 °C. However, the selectivity to MF decreases with the increase of temperature; at a temperature above 100 °C, the selectivity to MF drops dramatically and carbon dioxide turns out to be a major product. Meanwhile, Fig. S6 clearly illustrates that the activity of the Au–Pd/Gr–CNT catalyst in methanol oxidation is related to

the Gr/CNT ratio of Gr–CNT support; a Gr/CNT mass ratio of 5 gives the Au–Pd/Gr–CNT catalysts the best doping effect and the highest activity in methanol oxidation. The Au–Pd/Gr–CNT(5) catalyst with a Gr/CNT mass ratio of 5 exhibits much higher activity for methanol oxidation at low temperature than other Gr–CNT hybrids or graphene supported Au–Pd catalysts.

**{Fig. S6}**

A comparison of the catalytic performances in methanol oxidation among Au–Pd/Graphene, Au–Pd/Gr–CNT(5), and Au–Pd/Graphene + CNT (a physical mixture of Au–Pd/Graphene and CNT, with the same composition as Au–Pd/Gr–CNT(5)) is displayed in Fig. S7. As the pure supports (CNT, Graphene, Gr–CNT) are inert for the methanol oxidation, the catalytic performance of Au–Pd/Graphene + CNT mixture is almost identical to that of Au–Pd/Graphene, both are much poorer than Au–Pd/Gr–CNT(5). This suggests that it is impossible to insert CNT effectively into the graphene layers through later mechanical mixing. The promoting effect of CNT on the Au–Pd/Gr–CNT(5) catalyst may only appear when Au–Pd species are supported on the 3D Gr–CNT hybrid, where CNTs are uniformly inserted into the graphene layers through the solution self-assemble method.

**{Fig. S7}**

The catalytic activity of Au–Pd/Gr–CNT(5) is also compared with those of some similar catalysts recently reported for methanol oxidation to MF in the literature,[11–14] as given in Table S3. Although there are many factors that may influence the catalytic performance of a supported catalyst, the nature of support plays an important role in determining the catalyst activity. Table S3 suggests that Au–Pd/Gr–CNT(5), i.e. Au–Pd supported on 3D Gr–CNT hybrid, exhibits higher activity in the selective oxidation of methanol to MF at low

temperature, in comparison with those similar catalysts reported recently.

**{Table S3}**

Current results indicate that the incorporation of CNT into graphene as a spacing inserter is effective to inhibit the face to face aggregation of graphene sheets, bridge the defects for electron transfer and stabilize the hybrid three-dimensional structure. As a result, the dispersion of Au–Pd bimetallic particles, the synergy between Au and Pd and the strong interaction between Au–Pd particles and graphene support are enhanced greatly, which endow the Au–Pd/Gr–CNT catalyst high activity in methanol oxidation. Moreover, such an approach may be also effective to get highly active catalysts with graphene as support for other applications.

**Notes and references**

1   C. Chen, Q. Yang, Y. Yang, W. Lv, Y. Wen, P. Hou, M. Wang and H. Cheng, *Adv. Mater.*, 2009, **21**, 3007–3011.

2   W. Lv, D. Tang, Y. He, C. You, Z. Shi, X. Chen, C. Chen, P. Hou, C. Liu and Q. Yang, *ACS Nano*, 2009, **3**, 3730–3736.

3   R. Wang, Z. Wu, C. Chen, Z. Qin, H. Zhu, G. Wang, H. Wang, C. Wu, W. Dong, W.

Fan and J. Wang, *Chem. Commun.*, 2013, **49**, 8250–8252.

4   X. J. Niu, J. Gao, Q. Miao, M. Dong, G. F. Wang, W.B. Fan, Z. F. Qin and J.G. Wang, *Micropor. Mesopor. Mater.*, 2014, **197**, 252–261.

5   C. Chen, Q. Zhang, M. Yang, C. Huang, Y. Yang and M. Wang, *Carbon*, 2012, **50**, 3572–3584.

6   C. Xu, X. Wang and J. Zhu. *J. Phys. Chem. C*, 2008, **112**, 19841–19845.

7   D. Bulushev, I. Yuranov, E. Suvorova, P. Buffat and L. Kiwi-Minsker, *J. Catal.*, 2004, **224**, 8–17.

8   A. Venezia, L. Liotta, G. Pantaleo, V. La Parola, G. Deganello, A. Beck, Zs. Koppány, K. Frey, D. Horváth and L. Guczi, *Appl. Catal., A*, 2003, **251**, 359–368.

9   G. Wu, X. Wang, N. Guan and L. Li, *Appl. Catal., B.*, 2013, **136–137**, 177–185.

10  R. Lv, T. Cui, M. Jun, Q. Zhang, A. Cao, D. Su, Z. Zhang, S. Yoon, J. Miyawaki, I. Mochida and F. Kang, *Adv. Function. Mater.*, 2011, **21**, 999–1006.

11  L. Merte, M. Ahmadi, F. Behafarid, L. Ono, E. Lira, J. Matos, L. Li, J. Yang and B. Cuenya, *ACS Catal.*, 2013, **3**, 1460–1468.

12  A. Wittstock, V. Zielasek, J. Biener, C. Friend and M. Baumer, *Science*, 2010, **327**, 319–322.

13  G. Whiting, S. Kondrat, C. Hammond, N. Dimitratos, Q. He, D. Morgan, N. Dummer, J. Bartley, C. Kiely, S. Taylor and G. Hutchings, *ACS Catal.*, 2014, **4**, 637–644.

14  R. Wojcieszak, M. Ghazzal, E. Gaigneaux and P. Ruiz, *Catal. Sci. Technol.*, 2014, **4**, 738–745

**Table S1.** Actual loadings of Au and Pd on different Au–Pd catalysts determined by ICP-AES

| Catalyst | Au loading (wt.%) | Pd loading (wt.%) |
|---|---|---|
| Au–Pd/CNT | 1.90 | 0.84 |
| Au–Pd/Graphene | 1.80 | 0.76 |
| Au–Pd/Gr–CNT(1) | 2.00 | 0.91 |
| Au–Pd/Gr–CNT(3) | 1.96 | 0.89 |
| Au–Pd/Gr–CNT(5) | 1.89 | 0.83 |

**Table S2.** Quantitative analysis results from XPS and XAFS measurements for Au–Pd nano particles supported on CNT, graphene and Gr–CNT [a]

| Catalyst | Pd $3d_{5/2}$, BE($A$) (eV) [a] | | Pd $3d_{3/2}$, BE($A$) (eV) [a] | | Pd$^0$ fraction (%) | |
| --- | --- | --- | --- | --- | --- | --- |
| | Pd$^0$ | Pd$^{2+}$ | Pd$^0$ | Pd$^{2+}$ | By XPS [b] | By XAFS [b] |
| Au–Pd/CNT | 355.6(623) | 338.3(513) | 340.8(366) | 343.2(201) | 58.0 | -- |
| Au–Pd/Graphene | 355.6(1323) | 338.1(886) | 340.9(1150) | 344.2(1007) | 56.7 | 61.3 |
| Au–Pd/Gr–CNT(1) | 355.4(963) | 337.9(858) | 340.7(943) | 343.7(848) | 52.8 | -- |
| Au–Pd/Gr–CNT(3) | 355.3(3477) | 337.4(1966) | 340.7(2191) | 343.1(1520) | 62.0 | -- |
| Au–Pd/Gr–CNT(5) | 355.2(2571) | 337.1(1055) | 340.5(1770) | 343.0(1048) | 67.3 | 75.0 |

[a] BEs are the binding energies of each peak fitted from the XPS spectra; the numerals in the parenthesis are the relative areas ($A$) of each peak.

[b] The fraction of Pd$^0$ determined by XPS is calculated as

$$\left(A_{\mathrm{Pd^0-3d_{5/2}}} + A_{\mathrm{Pd^0-3d_{3/2}}}\right)/\left(A_{\mathrm{Pd^0-3d_{5/2}}} + A_{\mathrm{Pd^0-3d_{3/2}}} + A_{\mathrm{Pd^{2+}-3d_{5/2}}} + A_{\mathrm{Pd^{2+}-3d_{3/2}}}\right).$$

[c] The fraction of Pd$^0$ determined by XAFS is calculated through linear fitting by IFEFFIT software.

**Table S3.** A comparison of the catalytic activity of Au–Pd/Gr–CNT(5) with those of some similar catalysts reported in the literature.

| Catalyst | Temperature (°C) | $x_{MeOH}$ (%) | $s_{MF}$ (%) | TOF ($h^{-1}$) | Ref. |
|---|---|---|---|---|---|
| Pt/Al$_2$O$_3$ | 35 | 45.0 | 40.0 | 352 | 11 |
| nanoporous Au | 80 | 60.0 | 97.0 | 7.7 | 12 |
| Au–Pd/TiO$_2$ | 150 | 12.5 | 35.0 | 8.1 | 13 |
| Pd/SiO$_2$ | 80 | 88.0 | 72.0 | 226 | 14 |
| Au–Pd/Gr–CNT(5) | 45 | 42.5 | 100 | 150 | this work |

Note: Turnover frequency (TOF), the number of methanol molecules converted to MF per active site and hour, is estimated on basis of total Au and Pd atoms.

**Captions**

**Table S1.** Actual loadings of Au and Pd on different Au–Pd catalysts determined by ICP-AES.

**Table S2.** Quantitative analysis results from XPS and XAFS measurements for Au–Pd nano particles supported on CNT, graphene and Gr–CNT.

**Table. S3.** A comparison of the catalytic activity of Au–Pd/Gr–CNT(5) with those of some similar catalysts reported in the literature.
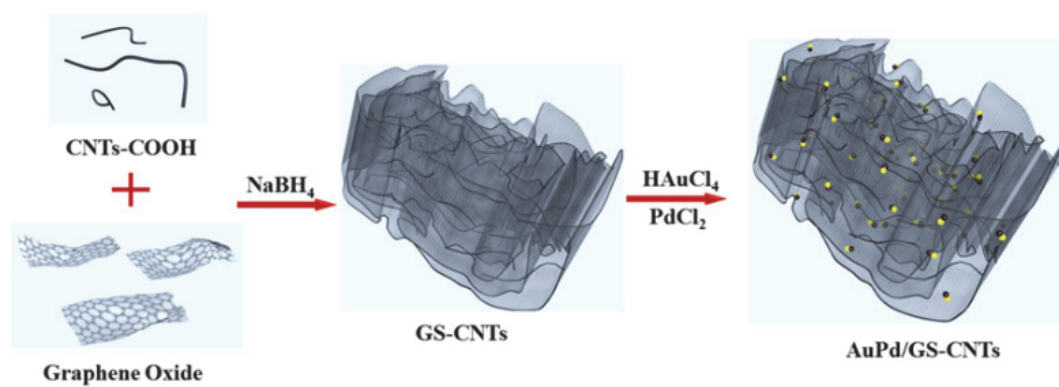
**Fig. S1.** Schematic diagram for the preparation of Au–Pd/Gr–CNT nanocomposite catalysts.
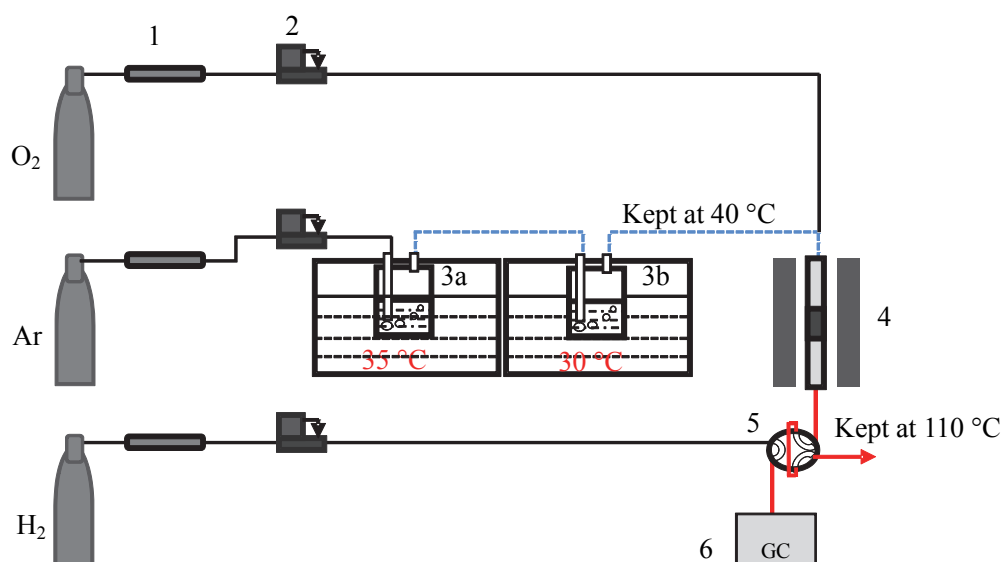
**Fig. S2.** Schematic setup of the apparatus for the catalytic tests of methanol selective oxidation: (1) Purification tube, (2) Mass flow controller, (3) Methanol saturator, (4) Fixed-bed reactor, (5) Six-way valve, and (6) Gas chromatograph.

**Fig. S3.** Nitrogen adsorption-desorption isotherms of (a) graphene, (b) Gr–CNT(1), (c) Gr–CNT(3), (d) Gr–CNT(5), and (e) Au–Pd/Gr–CNT(5).

**Fig. S4.** Enlarged HRTEM image of the Au–Pd/Gr–CNT(5) catalyst.

**Fig. S5.** SEM images of (a) Au–Pd/Gr–CNT(1), (b) Au–Pd/Gr–CNT(3), and (c) Au–Pd/Gr–CNT(5) and the EDX spectra of (d) Au–Pd/Gr–CNT(5).

**Fig. S6.** Conversion of methanol (I) and selectivity to MF (II) along with the reaction temperature for methanol oxidation over Au–Pd nanoparticles supported on Gr–CNT hybrids with different Gr/CNT ratios: (a) Au–Pd/Gr–CNT(1), (b) Au–Pd/Gr–CNT(3), (c) Au–Pd/Gr–CNT(5), and (d) Au–Pd/Graphene. The loadings of Au and Pd for all supported

Au–Pd catalysts are 2 and 1 wt.%, respectively; the feed stream consists of 6.4 vol.% $CH_3OH$, 70.2 vol.% $O_2$, and balanced argon, with a gas hourly space velocity (GHSV) of 42,800 mL $g^{-1}$ $h^{-1}$.

**Fig. S7.** Conversion of methanol (I) and selectivity to MF (II) along with the reaction temperature for methanol oxidation over (a) Au–Pd/Gr–CNT(5), (b) Au–Pd/Graphene + CNT (a physical mixture of Au–Pd/Graphene and CNT, with the same composition as Au–Pd/Gr–CNT(5)), and (c) Au–Pd/Graphene. The feed stream consists of 6.4 vol.% $CH_3OH$, 70.2 vol.% $O_2$, and balanced argon, with a gas hourly space velocity (GHSV) of 42,800 mL $g^{-1}$ $h^{-1}$.

**Fig. S1.**



**Fig. S1.** Schematic diagram for the preparation of Au–Pd/Gr–CNT nanocomposite catalysts.

**Fig. S2.**



**Fig. S2.** Schematic setup of the apparatus for the catalytic tests of methanol selective oxidation: (1) Purification tube, (2) Mass flow controller, (3) Methanol saturator, (4) Fixed-bed reactor, (5) Six-way valve, and (6) Gas chromatograph.
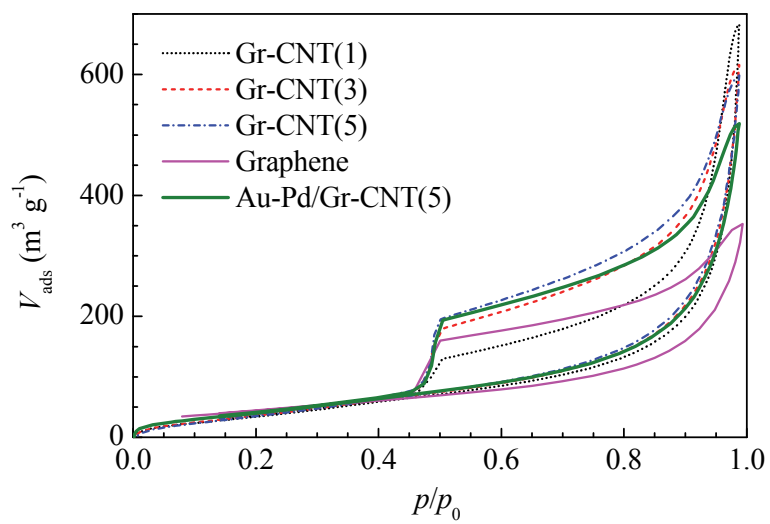
**Fig. S3.**



**Fig. S3.** Nitrogen adsorption-desorption isotherms of (a) graphene, (b) Gr–CNT(1), (c) Gr–CNT(3), (d) Gr–CNT(5), and (e) Au–Pd/Gr–CNT(5).

**Fig. S4.**



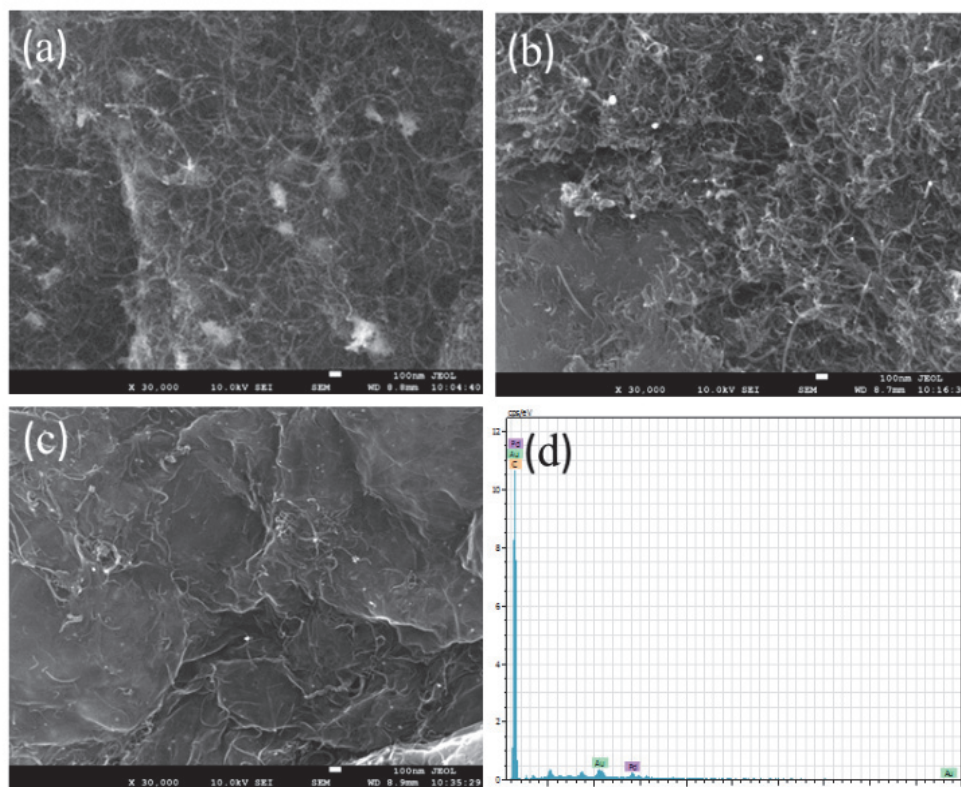**Fig. S4.** Enlarged HRTEM image of the Au–Pd/Gr–CNT(5) catalyst.

**Fig. S5.**



**Fig. S5.** SEM images of (a) Au–Pd/Gr–CNT(1), (b) Au–Pd/Gr–CNT(3), and (c) Au–Pd/Gr–CNT(5) and the EDX spectra of (d) Au–Pd/Gr–CNT(5).
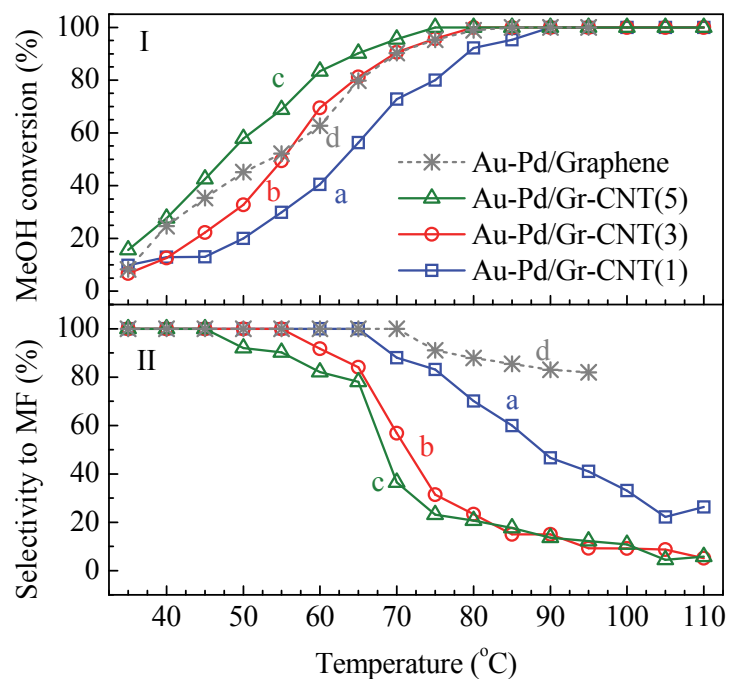
**Fig. S6.**



**Fig. S6.** Conversion of methanol (I) and selectivity to MF (II) along with the reaction temperature for methanol oxidation over Au–Pd nanoparticles supported on Gr–CNT hybrids with different Gr/CNT ratios: (a) Au–Pd/Gr–CNT(1), (b) Au–Pd/Gr–CNT(3), (c) Au–Pd/Gr–CNT(5), and (d) Au–Pd/Graphene. The loadings of Au and Pd for all supported Au–Pd catalysts are 2 and 1 wt.%, respectively; the feed stream consists of 6.4 vol.% $CH_3OH$, 70.2 vol.% $O_2$, and balanced argon, with a gas hourly space velocity (GHSV) of 42,800 mL $g^{-1}$ $h^{-1}$.
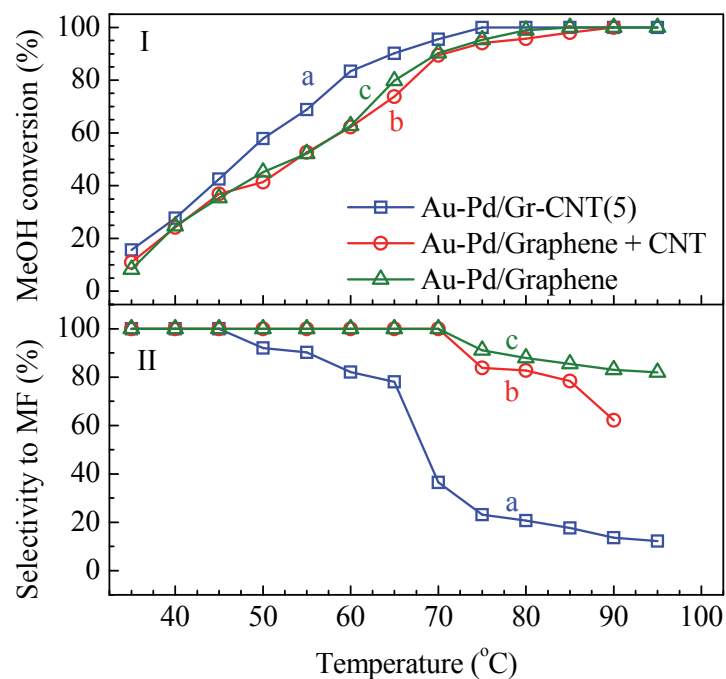
**Fig. S7.**



**Fig. S7.** Conversion of methanol (I) and selectivity to MF (II) along with the reaction temperature for methanol oxidation over (a) Au–Pd/Gr–CNT(5), (b) Au–Pd/Graphene + CNT (a physical mixture of Au–Pd/Graphene and CNT, with the same composition as Au–Pd/Gr–CNT(5)), and (c) Au–Pd/Graphene. The feed stream consists of 6.4 vol.% $CH_3OH$, 70.2 vol.% $O_2$, and balanced argon, with a gas hourly space velocity (GHSV) of 42,800 mL $g^{-1}$ $h^{-1}$.